Quantum evolution of a chaotic system in contact with its surroundings

Shanta Chaudhuri, Devashis Majumdar, and Deb Shankar Ray
Indian Association for the Cultivation of Science, Jadavpur, Calcutta 700 032, India
(Received 27 July 1995; revised manuscript received 27 November 1995)

Making use of appropriate quantum-classical correspondence we have examined the differential behavior of regular and chaotic trajectories in terms of quantum decoherence, the evolution of average quantities, and variances and entropy in a driven double-well oscillator in contact with the surroundings. Our numerical analysis has shown that even on a short time scale the decay of the average quantum coherence is multiexponential. While the onset of decoherence is much faster for a regular trajectory, the decay is faster asymptotically for a chaotic trajectory compared to a regular one. The coupling of the system to the environment turns chaotic in a regular evolution. The environment also affects the evolution of quantum variances for a regular trajectory almost from the beginning, while it has an insignificant effect on chaotic evolution up to a time after which, for both trajectories, noise in the quantum variances exhibits remarkable suppression, although fluctuations of the reservoir modes, in general, tend to increase the level of variances. We identify three stages of quantum evolution; a short decoherence regime followed by a Liouville flow, the latter regime being dominated by the classical curvature of the potential. This is the regime at which growth of entropy or quantum variances is exponential, the rate being determined by the classical largest Lyapunov exponent. The last stage is the irreversible flow dominated by diffusion which suppresses noises in the quantum variances. [S1063-651X(96)11305-2]

PACS number(s): 05.40.+j, 05.45.+b, 03.65.Bz

I. INTRODUCTION

It is well known that the evolution of a quantum system may be profoundly affected by its surroundings [1–8]. For this, a low-dimensional dynamical system weakly interacting with an environment which encompasses a virtually infinite number of degrees of freedom has been the standard paradigm in a wide range of physical disciplines, e.g., in chemical physics, quantum optics, solid state physics, etc. The problems of activated barrier crossing [9] and dissipative quantum tunneling [10] are well known examples in this context. Although effects due to environment on the dynamics are well accounted for in this model, nonlinear features are suppressed in these treatments because of the traditional linearized schemes employed to describe the dynamics within the well or around the barrier top. A nonlinear system which admits chaotic behavior in the classical version of the model, and which at the same time is coupled to an environment, is therefore worthy of investigation for studying the relationship between classical and quantum evolution. The coupling of the system with its surroundings induces an exchange of energy between them, resulting in a dissipation of the energy of the system. This was the subject of early studies of a dissipative standard map and other models by Dittrich and Graham and others [2,3]. Also, the incoherent interaction of the system with the environment results in a loss of phase coherence between the set of preferred quantum states in the Hilbert space of the system, thereby causing decoherence and classicality in the quantum system. The study of this quantum decoherence or interference effect has proved to be useful in a further analysis of quantum-classical correspondence by Zurek and Paz [6] (ZP) in an inverted harmonic oscillator potential. Although it is integrable in nature, and quantum corrections due to nonlinearity are absent, the model captures some essential features of decoherence in relation to quantum evolution around the hyperbolic classical orbit. The quantum decoherence in circle and stadium billiards has also been the subject of a recent study by Tameshtit and Sipe [7] (TS).

It is the purpose of the present paper to examine the differential behavior of the chaotic and regular trajectories, and the quantum-classical correspondence in a truly chaotic system (where the linearization scheme around the stable or unstable fixed point has not been employed) coupled to an environment. Since the strength and nature of coupling play a crucial role in setting the decoherence and its time scale, we have chosen the high temperature situation of an Ohmic environment keeping the relaxation rate very small but finite. The quantum-mechanical description of dissipation by now constitutes a well developed body of theory [11,12], and it can be incorporated without difficulty into the model for chaotic dynamics considered by us.

We thus construct a dissipative version of a model-driven double-well oscillator to study the evolution of a quantum system in the presence of weak dissipation and strong diffusion of fluctuations from the reservoir modes. We design the initial conditions in terms of minimum uncertainty wave packets to maximize the classical quantum correspondence. We show that the decay of average decoherence as measured by Tr ρ^2 is multiexponential. While the onset of decoherence is much faster for a regular trajectory, the decay is faster asymptotically for the chaotic trajectory compared to the regular one. The coupling of the system to the environment turns chaotic evolution into regular evolution, leading to some kind of weak localization at the barrier top. The environment also affects the evolution of quantum variances for a regular trajectory almost from the beginning while it has an insignificant effect on chaotic evolution up to a time after which for both trajectories noise in quantum variances exhibits remarkable suppression, although, in general, the fluctua-

tions of the reservoir modes tend to increase the level of variances to a significant extent.

Before concluding this section we emphasize some important points: First, the model employed in the present study is a generalized version of the model employed for the quantum Kramer's problem [9], where one encounters the case of an activated barrier crossing. The model can also be viewed as a generalization of a model that is extensively used for the problem of dissipative quantum tunneling [10] which essentially concerns barrier penetration in the presence of dissipation. For both these problems the model oscillator remains undriven, which renders the uncoupled system integrable. Second, studies on dissipative chaotic systems carried out so far were mostly based on maps. The present treatment is free from the linearization scheme and is a numerical simulation of this kind on a continuous system where we do not invoke any *ad hoc* separation of the time scale between the population and coherence dynamics, and take both dissipation and diffusion on an equal footing. Third, the present numerical experiment should serve to complement some of the earlier theoretical findings of Zurek and Paz.

The organization of the paper is as follows: In Sec. II we introduce the model system coupled to the environment, and describe its density operator in terms of the master equation which governs the temporal evolution. In subsequent sections we present our representative numerical results. In Sec. III we characterize the coherence of the quantum system in terms of purity, and then in Sec. IV study the evolution of the Husimi function and entropy. The evolution of average quantities has been described in Sec. V. Section VI deals with quantum variances, and shows how they differ for chaotic and regular trajectories. The paper is concluded in Sec. VII.

II. DISSIPATIVE CHAOTIC DYNAMICS: MODEL AND MASTER EQUATION

To start with, we consider a classically chaotic system characterized by a potential

$$V(x)=ax^4-bx^2+gx\,\cos(\omega_0 t),$$

where the first two terms comprise the double-well oscillator which is driven by a classical oscillating field as denoted by the third term. g includes the effect of strength of the field of frequency ω_0 and the coupling. The Hamiltonian for the system is given by

$$H_0=p^2/2m+V(x), \tag{1}$$

where the first term refers to the kinetic energy of the oscillator.

For this classical model [12,13] the parameter values $m=1$, $a=0.5$, $b=10.0$, $g=10.0$, and $\omega_0=6.07$ typically yield a chaotic zone for the initial condition $x=-3.5$ and $p=0.0$, and regular trajectories starting from $x=-2.0$ and $p=0.0$ or $x=-4.224$ and $p=0.0$, etc. While the regular trajectories remain confined in the respective wells, the chaotic trajectories spread out over the two wells. Classical and quantum-mechanical studies on this model have been made earlier in the context of tunneling [13] and barrier crossing [14].

The bare system is now coupled to an environment modeled by a reservoir of harmonic oscillator modes [11,12]. With the Hamiltonian of the driven double-well oscillator, the generator of the quantum dynamics is given by the overall Hamiltonian operator for the system and the environment and their coupling,

$$\hat{H}=\hat{H}_0+\hbar\sum_i\ \omega_i\hat{b}_i^\dagger\hat{b}_i+\hbar\sum_i\ [k(\omega_i)\hat{b}_i+k^*(\omega_i)\hat{b}_i^\dagger]\hat{x}, \tag{2}$$

where $\hat{x}$ and $\hat{p}$ become position and momentum operators of the system. $\hat{b}_i$ ($\hat{b}_i^\dagger$) denotes the annihilation (creation) operator of the harmonic oscillator bath modes. The second and third terms correspond to reservoir modes and their coupling to the chaotic system. Also note that $k(\omega_i)$ is a c function.

It is convenient to invoke the rotating wave approximation, so that one can use a symmetric coupling of the type $(\hat{b}_i\hat{a}^\dagger+\hat{b}_i^\dagger\hat{a})$, where a and $a^\dagger$ are annihilation and creation operators corresponding to the system, respectively, as given by $x=1/\sqrt{2m\omega}(\hat{a}+\hat{a}^\dagger)$. ω refers to the frequency of the harmonic oscillator, on the basis of which the quantum calculation is performed as described in the latter part of this section.

Appropriate elimination of reservoir modes in the usual way [11,12], using Born and Markov approximations, leads us to the following reduced density matrix equation for the evolution of the system:

$$\frac{d\hat{\rho}}{dt}=-(i/\hbar)[\hat{H}_0,\hat{\rho}]+(\gamma/2)(\hat{a}\hat{a}^\dagger\hat{\rho}-2\hat{a}\hat{\rho}\hat{a}^\dagger+\hat{\rho}\hat{a}^\dagger\hat{a})$$
$$+D(\hat{a}^\dagger\hat{\rho}\hat{a}+\hat{a}\hat{\rho}\hat{a}^\dagger-\hat{a}^\dagger\hat{a}\hat{\rho}-\hat{\rho}\hat{a}\hat{a}^\dagger). \tag{3}$$

Here the spectral density function of the reservoir is replaced by a continuous density $g(\omega)$; we denote the Boltzmann constant by k, and $\gamma>0$ is the limit of $2\pi|k(\omega)|^2g(\omega)/\omega$ as $\omega\to 0_+$ and is assumed to be finite. γ is the relaxation rate, $D(=\overline{n}\gamma)$ is the diffusion coefficient, and $\overline{n}$ $(=[\exp(\hbar\omega/kT)-1]^{-1})$ is the average thermal photon number. In the high temperature limit $D\cong\gamma kT/\hbar\omega$. Terms analogous to Lamb and Stark shifts have been neglected, and temperature T is assumed to be high enough for the Markov approximation to be valid.

The first term in Eq. (3) which corresponds to the free and classically driven motion of the oscillator generates the ordinary Liouville flow. The terms containing γ arise due to interaction with the environment. The first of them implies the relaxation or exchange of energy with the reservoir, and the last one indicates the diffusion of fluctuations of the reservoir modes into the system of interest. The last term is responsible for the quantum decoherence process.

To solve Eq. (3) it is convenient to choose as basis vectors the eigenvectors $\{|n\rangle\}$ of a harmonic oscillator $(\hat{p}^2/2m+\frac{1}{2}m\omega^2\hat{x}^2)|n\rangle=[n+\frac{1}{2}\hbar\omega|n\rangle$. The frequency ω of the harmonic oscillator is arbitrary, and it can be adjusted to economize the basis functions. For the present purpose we choose $\omega=6.25$ and $\hbar=1$, and use 120 basis vectors. In this representation the equation of motion for the reduced density matrix elements is given by

$$\frac{d\rho_{nm}}{dt} = -i\left\{\sum_k H_{nk}\rho_{km} - \sum_l \rho_{nl}H_{lm}\right\} + \gamma/2\{\sqrt{(n+1)(m+1)}\rho_{n+1\ m+1} - (n+m)\rho_{nm}\} + D\{\sqrt{(n+1)(m+1)}\rho_{n+1\ m+1} - (n+m+1)\rho_{nm}\}. \tag{4}$$

The expression for matrix elements H_{mn} may be found in Ref. [13]. Equation (4) describes the evolution of both population (diagonal elements) and coherences (off-diagonal elements). Without resorting to any approximate scheme for separation of time scales to show their evolution, we carried out a numerical solution of 120×120 equations for density matrix elements of the reduced system as a typical initial value problem. We follow the stroboscopic time scale, i.e., the period of driving force $T=2\pi/\omega_0$, so that $t=nT$.

To bring forth a quantum-classical correspondence, we construct minimum uncertainty wave packets $|\alpha_{x,p}\rangle$ of a Gaussian form in position and momentum representations having average position $\langle x\rangle$ and average momentum $\langle p\rangle$, such that

$$\langle \alpha_{x,p}|n\rangle = [\exp(-0.5|\alpha|^2)]\alpha^n/\sqrt{n!}.$$

Here we denote $\alpha=\sqrt{m\omega/2}(\langle x\rangle + (i/m\omega)\langle p\rangle)$ and set the initial condition for quantum evolution by fixing the average position and average momentum of the wave packet corresponding to the initial position and momentum of a classical trajectory.

In our analysis we specifically consider a high temperature environment. We choose the relaxation rate γ to a very small (0.001) compared to the diffusion rate $D(=0.5)$ by keeping T large, the relation between the two being given by $D=\bar{n}\gamma$. This last relation implies that the average thermal photon number $\bar{n}=500$. In the standard cavity quantum electrodynamic problems [15], where superconducting high-Q cavities are used, the average thermal photon number, may, however, be reduced even several orders of magnitude lower. In this dynamical problem (which is reminiscent of cavity QED) one is thus essentially concerned with a number of competing processes, e.g., the fundamental strong coherent interaction (g) between the double-well oscillator and the external classical field (strong coupling being responsible for chaos in the classical counterpart), spontaneous decay of oscillator (γ), and the thermal-field-induced stimulated processes (D), the latter two processes being treated in the weak coupling scheme. We thus consider the high temperature environment in the limit $g\gg D\gg\gamma$. It is well known that most often in the process of thermalization the temporal evolution of the density matrix proceeds in two stages. The decoherence occurs in the first stage, which is then followed by relaxation on a much longer time scale. We have studied quantum evolution for a number of regular and chaotic trajectories. However, for the sake of brevity here we present the results of a numerical simulation for typical single regular and chaotic trajectories. As a numerical check we compared our numerical results with those of Lin and Ballentine [13] in classical and quantum cases for $D=0$ and $\gamma=0$. Another important check for numerical calculations is to keep $\mathrm{Tr}\,\rho=1$ for the entire evolution.

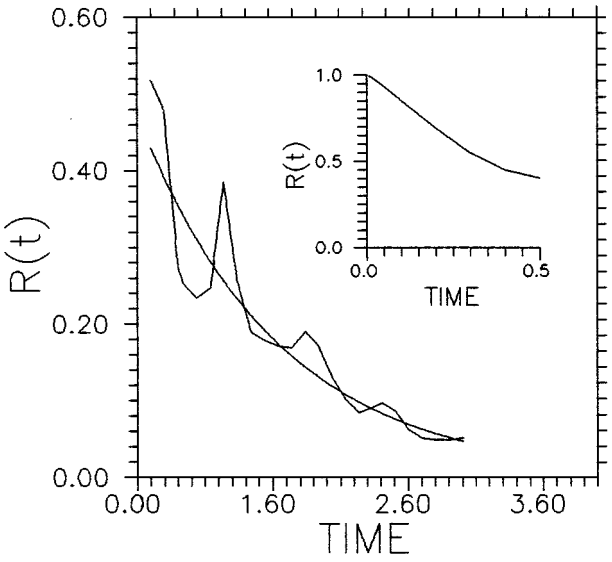

FIG. 1. Plot of $\mathrm{Tr}\,\rho^2$ $[R(t)]$ vs time for a chaotic trajectory starting from $\langle x\rangle=-3.5$ and $\langle p\rangle=0.0$ (the exponential curve is the best fit curve). The inset shows the onset of decay of $\mathrm{Tr}\,\rho^2$ for the same trajectory for time up to 0.5. (Both the units are arbitrary.)

Before bringing an end to this section we emphasize that, although we compare our numerical results with the recent theoretical finding of ZP wherever possible, it is not completely within the scope of this theory for the reason that the model of an inverted harmonic oscillator as employed by ZP, though it mimics some features of a hyperbolic fixed point, is integrable, and features due to nonlinearity are absent. In the absence of any mathematical treatment which goes beyond the linearization scheme, we think that our numerical observations as presented in the next few sections will be complementary to that of the earlier theoretical finding of ZP.

III. QUANTUM DECOHERENCE

The concept of coherence in quantum-mechanical systems has been advocated in a number of different ways [5,7,8]. If the system evolves in contact with a thermal reservoir from an initially pure state, it is convenient to define a measure of coherence in terms of purity of the state or average coherence as

$$R(t)\equiv \mathrm{Tr}\,\hat{\rho}(t)^2.$$

If the system is in a pure state, then $\mathrm{Tr}\,\rho^2=\mathrm{Tr}\,\rho=1$ or $R=1$. The loss of purity or mixing implies $R(t)<1$. Thus we have $0\leqslant R\leqslant 1$.

In Figs. 1 and 2 we display the decay of quantum coherence as measured by $R(t)$ as a function of time. It is apparent that even within a very short time, decoherence proceeds typically in two stages. Figure 1 depicts the case of a wave packet which is located at $x=-3.5$ and $p=0.0$ (corresponding to a classically chaotic trajectory). The multiexponential decay curve suggests two time scales. The inset in Fig. 1 shows short time behavior, with a rate constant approximately equal to 1.96, while the long time behavior characterized by a rate constant almost half of that for the short time scale is shown in Fig. 1 (0.96). Biexponential decay of

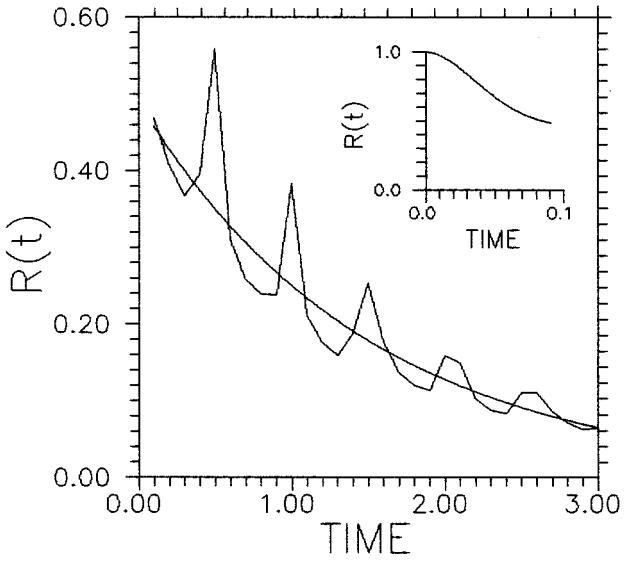

FIG. 2. Same as Fig. 1 but for a regular trajectory starting from $\langle x\rangle=-2.0$, $\langle p\rangle=0.0$. The exponential curve is the best fit curve. The inset shows the onset of decay of Tr ρ^2 for the same trajectory for time up to 0.1. (Both the units are arbitrary.)

coherence is also apparent for a typical regular trajectory, as shown in Fig. 2. The inset in Fig. 2 exhibits the fastest time scale for the initial stage of decoherence (the rate constant $\cong 9.4$) which is followed by an order of magnitude slower decoherence process (the rate constant $\cong 0.67$). It is thus interesting to note that the time scale for the onset of decoherence is much faster for a regular rather than for a chaotic trajectory, although in the latter stage the loss of coherence proceeds asymptotically at a faster rate for a chaotic trajectory than for a regular one.

It is important to mention at this point that the problem of decoherence has been studied earlier by ZP [6] and TS [7,8] in a high temperature Ohmic environment. In the case of decoherence studied by TS, coupling to the heat bath is of quantum nondemolition type, implying that the weak perturbation commutes with the system Hamiltonian, and average coherence was found to decay faster asymptotically in the chaotic system than in the regular system. This is a direct result of the repulsion of energy levels in the former case. In the present case, however, the onset of decoherence is faster in the regular case, while asymptotic decoherence is faster in the chaotic case, similar to the case studied by TS. This may be understood in the following way.

There are two competing processes affecting the evolution of quantum coherence as measured by Tr ρ^2. One is the Liouville flow, the other is the diffusion. For a chaotic trajectory the Liouville flow is associated with an exponential expansion in one direction and a contraction along the other direction, so that a quasiprobability distribution function is squeezed. Diffusion, on the other hand, which is the main reason for decoherence, induces a spreading of the wave packet. This opposes the exponential contraction but has little effect on the exponential expansion. Thus decoherence is likely to be more opposed for a chaotic evolution than for a regular one. This explains the faster onset of decoherence for a regular evolution, at least in the initial stage before diffusive growth completely takes over the dynamics.

IV. EVOLUTION OF ENTROPY

Next we consider the evolution of a classical-like distribution corresponding to a Husimi function defined as

$$P(x,p)=1/2\pi\hbar\langle\alpha_{x,p}|\hat{\rho}|\alpha_{x,p}\rangle,$$

which provides a coarse-grained phase space smooth on a scale of $\hbar$. In Fig. 3(a) we choose the initial state $|\alpha_{x,p}\rangle$ centered at $x=-2.0$, $p=0.0$ (corresponding to a regular trajectory). The evolution of the Husimi function at time $t=3.06T$ and $8.26T$ is shown in Figs. 3(b) and 3(c), respectively. In contrast to the case of coherent tunneling, the Husimi function spreads rapidly, and shows no sign of recurrence. Quantum coherence is thus extremely susceptible to environmental effects.

To make our analysis of irreversible evolution more quantitative, it is useful to calculate the Von Neumann entropy H of the Gaussian state, which is related to the area σ enclosed by the contour of the Husimi function as defined by

$$H=k\ \ln(\sigma/\hbar).$$

In Fig. 4 we show the evolution of entropy for a regular (b) and a chaotic trajectory (a). In sharp contrast to the steady increase of entropy for the regular trajectory, the chaotic trajectory presents an interesting scenario. At a very early stage the entropy change remains very small, is then followed by a sharp increase, and then finally tends to increase at a very very slow rate. It is interesting to note that Zurek and Paz advocated the efficacy of studying the evolution of entropy as a consequence of the interplay between Liouville dynamics with the interaction of a high temperature environment to examine the differential behaviors of integrable and nonintegrable systems. In defining entropy ZP used the Wigner function (W), whereas we preferred to use the Husimi function. W is not always positive definite (it is therefore necessary to make use of a Gaussian smoothing of the Wigner function). The Husimi O'Connell-Wigner function [16] is positive definite, and for one degree of freedom takes the following form (we consider for illustration):

$$W_s(x,p)=\frac{1}{\hbar\pi}\int\int dx'dp'W(x',p')\exp\left[-\frac{\langle x'-x\rangle^2}{2\sigma^2}-\frac{(p'-p)^2}{2\beta^2}\right].$$

Here σ and β refer to widths of the Gaussian function. The Heisenberg principle implies that $\beta\sigma\geqslant\hbar/2$. The time evolution of W_s to lowest order in σ and β is given by

$$\frac{\partial W_s}{\partial t}=-\frac{p}{m}\frac{\partial}{\partial x}W_s+\frac{\partial V}{\partial x}\frac{\partial}{\partial p}W_s-\frac{\beta^2}{m}\frac{\partial^2 W_s}{\partial p\partial x}+2\sigma^2\left(\frac{\partial^2 V}{\partial x^2}\right)\frac{\partial^2 W_s}{\partial x\partial p}. \tag{5}$$

While the first two terms refer to the usual Poisson bracket term (classical motion), the third and fourth terms are due to Gaussian smoothing. According to O'Connell and Wigner

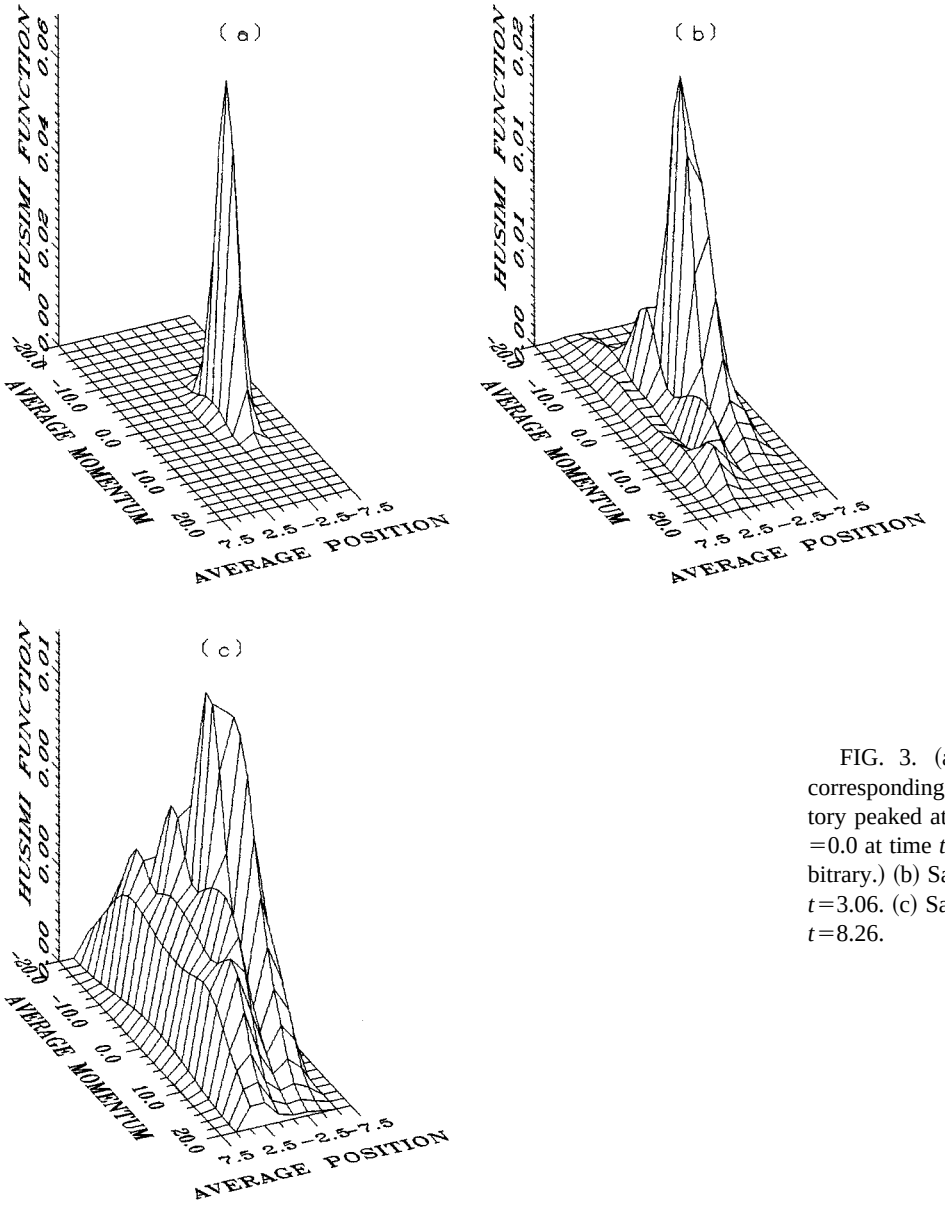

FIG. 3. (a) Husimi function corresponding to a regular trajectory peaked at $\langle x\rangle=-2.0$ and $\langle p\rangle=0.0$ at time $t=0.0$. (Units are arbitrary.) (b) Same as in (a) at time $t=3.06$. (c) Same as in (a) at time $t=8.26$.

[16] this is not, however, a quantum effect. It is evident from Eq. (5) that in addition to a momentum variance corresponding to β^2 there is a σ^2 effect due to coordinate variance. For a nonlinear potential, the term $\partial^2 V/\partial x^2$ contributes significantly to the spreading of the contour of the Husimi function. This curvature of the potential, $\partial^2 V/\partial x^2$, which is instrumental in determining the stability of the trajectory, controls the spreading of the coarse-grained phase space contour (note that for ZP this term is a constant). Thus in addition to the usual diffusive spreading due to the D term in Eq. (3) of type $D[(\partial^2/\partial x^2)+(\partial^2/\partial p^2)]$ we have spreading due to the β^2, $\sigma^2(\partial^2 V/\partial x^2)$ effect. The increase of entropy (the logarithmic function of the phase space contour) in the regular case is thus dependent only on the coupling to the bath, while in the chaotic case the rapid increase of the entropy is strongly dependent on the curvature of the potential. Recently we pointed out [17] that the Lyapunov exponent is related to the correlation between the fluctuations (due to classical chaos) of the curvature of the potential in the chaotic case. Since quantum variances in x and p diverge exponentially for the chaotic case [18], and the rate of growth is connected to the corresponding curvature of the potential and thereby to the largest classical Lyapunov exponent (see Ref. [19] for details), the initial growth of the phase space contour or entropy is exponential in nature. This can be checked simply by noting the parallel between the rapid growth of entropy and the uncertainty product (another measure of the increase in phase volume) (Figs. 4 and 11). It is thus apparent that just as the very early evolution is dominated by decoherence, the second stage of evolution is significantly influenced by the classical stability matrix or the curvature of the potential, and, quantitatively, the onset of entropy is controlled by the classical largest Lyapunov exponent. In this regime the nature of the trajectory itself (i.e., regular or chaotic) overwhelms the effect of the surroundings.

V. EVOLUTION OF AVERAGE QUANTITIES

Let us now look at the quantum evolution of average positions and momenta of the system in terms of a phase-space-

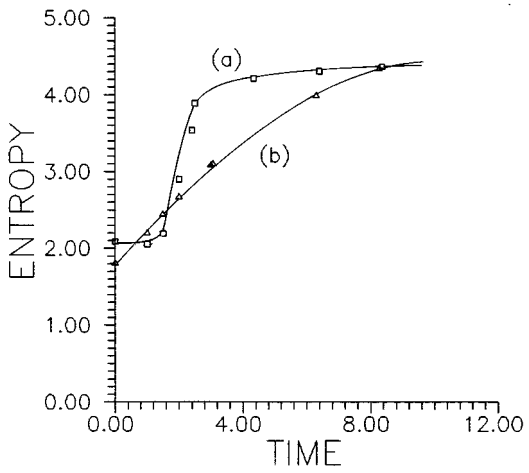

FIG. 4. Plot of entropy vs time. Curve (a) is for chaotic trajectory, and curve (b) is for the regular trajectory mentioned in the text. (Units are arbitrary.)

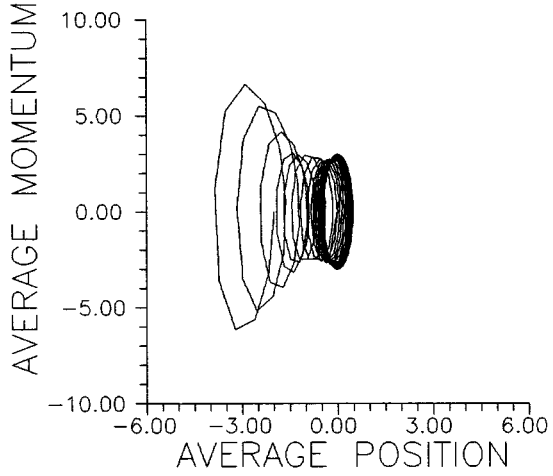

FIG. 6. Same as Fig. 5 but for $D=0.5$ and $\gamma=0.001$.

type plot. Figure 5 exhibits the case of a wave packet located initially at $x=-2.0$ and $p=0.0$ (corresponding to a classical regular trajectory) when the system is decoupled from the environment (i.e., $\gamma=0.0$ and $D=0.0$). It is apparent that the trajectory spirals around and moves from one well to the other. The coupling of the system to the environment ($\gamma=0.001$ and $D=0.5$) results in an inhibition of passage of the phase point or in coherent tunneling between the wells. After a few spirals the phase point settles down around the hyperbolic point (around the barrier top), as shown in Fig. 6. This behavior of the phase points is similar to what we observe for the environment-decoupled system for a chaotic trajectory starting at $x=-3.5$ and $p=0.0$ (Fig. 7). Here again the phase points remain largely confined in the vicinity of the hyperbolic point of the potential. Figure 8 shows the $\langle x\rangle$-$\langle p\rangle$ plot of the same trajectory for the system coupled to the environment. It is observed that the same dynamic localization at the barrier top persists.

We thus see that on coupling the system to the environment, whereby we introduce dissipation of energy from the system as well as diffusion of fluctuations from the reservoir modes into the system, the behavior of the wave packets initially localized at the position corresponding to classically regular or chaotic trajectories is different. We observe that coherent tunneling pertaining to the regular description is destroyed, and at the same time coupling turns a regular evolution chaotic, resulting in some kind of weak localization at the barrier top.

We now mention a few pertinent points regarding the notion of localization at this stage. The investigation of Hamiltonian systems with infinite-dimensional Hilbert space, e.g., the standard map, has revealed that classical chaotic behavior is suppressed on quantization. The suppression is due to interference effects of the number of modes accessible to the quantum system [20]. The situation is analogous to strong localization in tight-binding Hamiltonian systems [21]. This localization is extremely susceptible to destruction even by

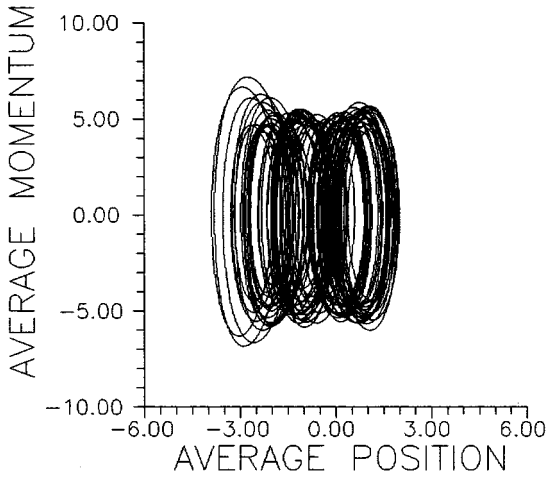

FIG. 5. Plot of the quantum mechanical average position ($\langle x\rangle$) vs quantum mechanical average momentum ($\langle p\rangle$) for a regular trajectory starting from $\langle x\rangle=-2.0$ and $\langle p\rangle=0.0$ and $D=0.0$ and $\gamma=0.0$. (Units are arbitrary.)

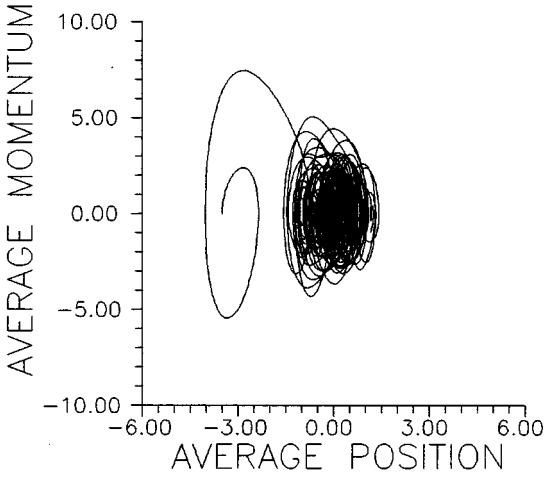

FIG. 7. Same as Fig. 5 but for a chaotic trajectory starting from $\langle x\rangle=-3.5$ and $\langle p\rangle=0.0$ when the system is not coupled to the environment ($D=0.0$ and $\gamma=0.0$).

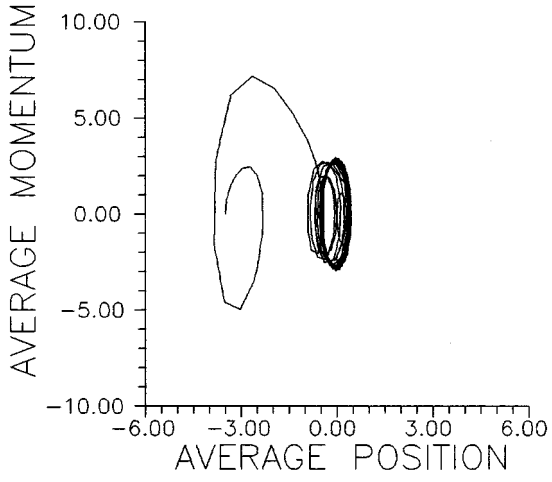

FIG. 8. Same as Fig. 7 but for $D=0.5$ and $\gamma=0.001$.

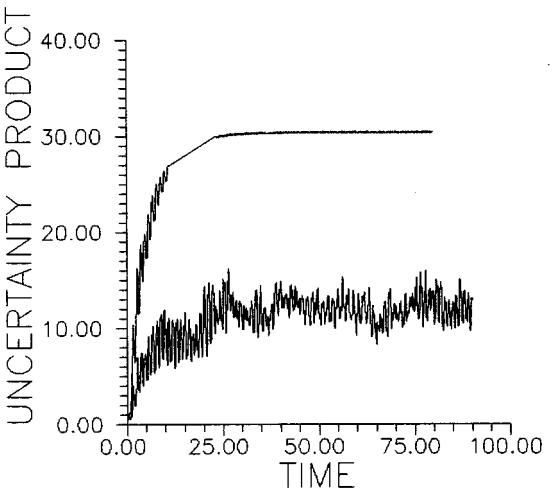

FIG. 9. Plot of the uncertainty product vs time for a regular trajectory starting from $\langle x\rangle=-2.0$ and $\langle p\rangle=0.0$. The lower curve is for the trajectory when $D=0.0$ and $\gamma=0.0$, and the upper curve is for the trajectory when $D=0.5$ and $\gamma=0.001$. (Both the units are arbitrary.)

weak dissipation [2], resulting in linear diffusion, which is the hallmark of chaotic behavior, and in the process classicality is restored. Localization at the barrier top of the double-well potential (undriven and driven by a constant field) has also been investigated as a stationary quantum problem [22]. We emphasize here that the dynamic localization around the barrier top for the chaotic trajectory for the system decoupled from the environment, as well as that for the trajectory coupled to the environment, are similar to what has been observed recently in an anharmonic driven chaotic oscillator (no environment) [23]. In contrast to strong localization, this weak localization [22] is not susceptible to weak dissipation or diffusion, is similar to what has been observed as weak localization in disordered systems, and is a manifestation of classical chaos on a time scale which is much shorter than the asymptotic time scale required to resolve the quasienergy levels of the system [23,24]. This seems to be an indication that chaos makes some properties more robust than expected against the influence of environmental fluctuations.

VI. QUANTUM FLUCTUATIONS

Quantum fluctuations are generic quantum effects. In the present problem we launched wave packets satisfying the minimum uncertainty product relation $\Delta x\Delta p=\hbar/2$. However, in the course of evolution the uncertainty product varies in time. In Fig. 9 we plot this variation for a regular trajectory starting at $x=-2.0$ and $p=0.0$, when the system is decoupled ($\gamma=0.0$, and $D=0.0$), and compare with the situation where the system is in contact with the heat bath ($\gamma=0.001$ and $D=0.5$). Switching on the coupling results in a large increase in the uncertainty product almost from the beginning. At almost $t\cong 30T$ the uncertainty product settles down at a constant value. Although the evolutionary trends in both cases are more or less similar, a closer look at Figs. 9 and 10 clearly reveals the level of noise in the quantum variances sharply drops at almost about $t\cong 11T$ for the system coupled to the environment. In Fig. 11 we plot the variation of the uncertainty product for a chaotic trajectory starting at $x=-3.5$ and $p=0.0$ for the coupled and bare systems. It is evident that unlike the regular trajectory the difference between the two situations is very small up to a time $t=11T$, after which the effect of the environment becomes remarkable. Along with the increase in the uncertainty as in the regular case there is a suppression of noise in the quantum variances. Comparing between the evolution of regular and chaotic trajectories of the uncoupled system, one also finds that quantum variances initially grow exponentially for the chaotic trajectory. This aspect has already been touched upon in Sec. IV for entropy, and can also be corroborated from other related investigations on kicked systems [19,18].

The origin of the differential behavior of quantum fluctuations for regular and chaotic trajectories can be summarized as follows. We first note that, after the decoherence stage is over, the dynamics is dominated by the Liouville flow. At this point, as discussed above, parallel with the observation that chaos creates an experimental growth of intrinsic fluctuations in classical systems, one finds that [19] quantum variances initially grow exponentially (this has been

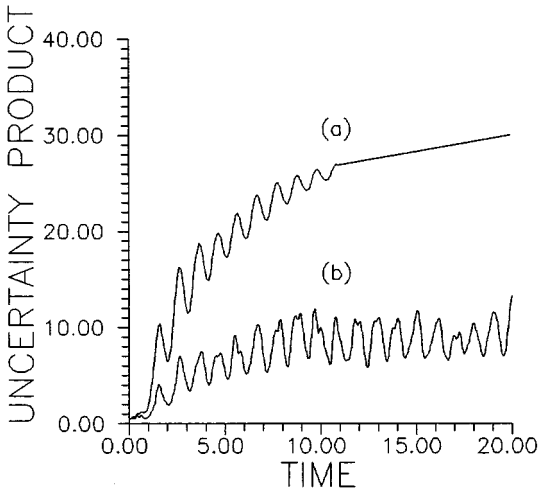

FIG. 10. Same as Fig. 9 but for time up to 20. Curve (*a*) is for $D=0.5$ and $\gamma=0.001$, and curve (*b*) is for $D=0.0$ and $\gamma=0.0$.

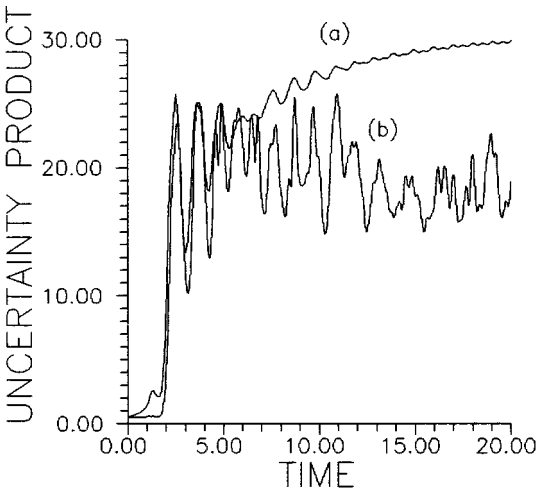

FIG. 11. Same as Fig. 10 but for a chaotic trajectory starting from $\langle x\rangle=-3.5$ and $\langle p\rangle=0.0$. Curve (*a*) is for $D=0.5$ and $\gamma=0.001$, and curve (*b*) is for $D=0.0$ and $\gamma=0.0$.

recognized as a generic signature of classical chaos on quantum phenomena) if the corresponding classical description is chaotic. The growth rate is controlled by fluctuations in the curvature of the potential, as pointed out above. At this stage fluctuations in the curvature of the potential dominate the evolution, which is then followed by an irreversible flow, where we find the suppression of noise in quantum variances. This reduction of noise (fluctuations in the quantum uncertainty) is probably due to damping of higher order quantum correlations.

Thus it is apparent that the environment affects the evolution of the regular trajectory almost from the beginning, whereas it has no noticeable effect on a chaotic trajectory up to a time after which, for both trajectories, noise in the quantum variances exhibits remarkable suppression. In general, the fluctuations of the reservoir modes tend to increase the level of uncertainty product.

Finally we mention that although both entropy and uncertainty product are related to the phase space contour, in the measurement of entropy we use a coarse-grained phase space. However, such coarse graining is absent in the calculation of the uncertainty product.

VII. SUMMARY: THREE STAGES OF QUANTUM EVOLUTION

Using an appropriate quantum-classical correspondence we have studied the effect of their surroundings on the quantum evolution of the average coherence, entropy, average quantities, and variances for classically chaotic and regular trajectories in a driven double-well system. The keypoint in taking the surrounding into account is to incorporate the fluctuation-dissipation relation in the Liouville dynamics. Although we have considered a high temperature situation, finite values of γ and D in the master equation ensure a balance between the outward energy flux from the system to the reservoir and the inward energy flux due to fluctuations of the reservoir modes into the system. Thus in the present treatment dissipation and diffusion have been treated on an equal footing. We note in passing that former considerations on related issues were based on specific limiting cases [2,6,8], such as $\gamma\rightarrow 0$ or $D\rightarrow 0$.

The high temperature situation has another implication. The dissipative part of the dynamics expressed through Eq. (3) is derived on the basis of the coupling of a harmonic oscillator (a system) to a reservoir of harmonic oscillators. The question of its general validity in the master equation (3), as applied to a nonlinear oscillator, naturally arises. It has been demonstrated [25,26] that in the high temperature situation, the description in terms of the dissipative dynamics is adequate even when the reservoir is coupled to a nonlinear oscillator, as in the present case.

To summarize our observations, we have shown that even on a short time scale the decay of average quantum coherence is multiexponential. While the onset of decoherence is much faster for a regular trajectory the decay is faster asymptotically for a chaotic trajectory compared to a regular one. An interplay of Liouville dynamics and diffusion is thus demonstrated. The effect of the surroundings is also sensitive enough to destroy a coherent tunneling of the wave packet. At the same time, the coupling of the system to the environment turns a regular trajectory chaotic, leading to some kind of weak localization at the barrier top. The environment also affects the evolution of quantum variances for a regular trajectory almost from the beginning, while it has no noticeable effect on the chaotic trajectory up to a time after which, for both trajectories, noise in the quantum variances exhibits a remarkable suppression, although, in general, the fluctuations of the reservoir modes tend to increase the level of quantum variances to a significant extent [27].

The differential behavior of the quantum evolution for regular and chaotic trajectories, as summarized above, suggests that one may identify three stages of quantum evolution as envisaged by Zurek and Paz in their investigation of unstable inverted harmonic oscillators. Quantum decoherence is the first stage of evolution, followed by the Liouville flow, a regime dominated by the curvature of the classical potential or the Jacobi matrix. In this regime the growth of entropy or quantum variances is exponential, the rate being determined by the classically largest Lyapunov exponent, and the differential behavior between the regular and chaotic trajectories is likely to be most prominent. The third stage of evolution is the irreversible flow largely dominated by diffusion. In this regime we observe the suppression of noise in quantum variances for both regular and chaotic trajectories, and the environment makes its presence felt exclusively. This observation of the suppression of noise also lends supports to the earlier assertion that openness in a quantum system induces classicality into it, a conclusion arrived at from different standpoints [2,6]. The present attempt is a detailed numerical simulation on this account, although the implications are too intricate for an immediate analytical treatment. In view of the prototypical role played by the present model in several earlier investigations, we hope that the conclusions drawn here will find qualitative applicability in other problems of dissipative dynamics in relation to classical and quantum chaos.

ACKNOWLEDGMENTS

Thanks are due to the Council of Scientific and Industrial Research for financial support to one of us (S.C.). D.S.R. is indebted to the Department of Science and Technology for partial financial support. The authors are thankful to Dr. G Gangopadhyay and Professor S. P. Bhattacharyya for interesting discussions and comments.

[1] T. Dittrich and R. Graham, Z. Phys. B **62**, 515 (1986).
[2] T. Dittrich and R. Graham, Ann. Phys. **200**, 363 (1990).
[3] R. Grobe and F. Haake, Z. Phys. B **68**, 503 (1987).
[4] W. H. Zurek, Phys. Rev. D **24**, 1516 (1981).
[5] E. Joos and H. D. Zeh, Z. Phys. B **59**, 229 (1985).
[6] W. H. Zurek and J. P. Paz, Phys. Rev. Lett. **72**, 2508 (1994); W. H Zurek, Phys. Today **44**(10), 36 (1991).
[7] X. Tameshtit and J. E. Sipe, Phys. Rev. A **47**, 1697 (1993).
[8] X. Tameshtit and J. E. Sipe, Phys. Rev. B **51**, 1582 (1995).
[9] P. Hanggi, P. Talkner, and M. Borokovec, Rev. Mod. Phys. **62**, 251 (1990).
[10] A. J. Leggett and A. O. Caldiera, Phys. Rev. Lett. **46**, 211 (1981).
[11] W. H. Louisell, *Quantum Statistical Properties of Radiation* (Wiley, New York, 1973).
[12] G. Gangopadhyay and D. S. Ray, in *Advances in Multiphoton Processes and Spectroscopy*, edited by S. H. Lin, A. A. Villayes, and F. Fujimura (World Scientific, Singapore, 1993), Vol. 8.
[13] W. A. Lin and L. E. Ballentine, Phys. Rev. Lett. **65**, 2927 (1990).
[14] S. Chaudhuri, G. Gangopadhyay, and D. S. Ray, Ind. J. Phys. **69B**, 507 (1995); Phys. Lett. (to be published).
[15] G. Gangopadhyay and D. S. Ray, Phys. Rev. A **43**, 6424 (1991); G. S. Agarwal, R. K. Bullough, and G. P. Hildred, Opt. Commun. **59**, 23 (1986). For experiments see, for example, D. Meschede, H. Walther, and G. Miller, Phys. Rev. Lett. **54**, 551 (1985).
[16] R. F. O'Connell and E. P. Wigner, Phys. Lett. **85A**, 121 (1981).
[17] S. Chaudhuri, G. Gangopadhyay, and D. S. Ray, Phys. Rev. A **47**, 311 (1993).
[18] In a number of numerical experiments it has been demonstrated that the initial growth of quantum variances for the chaotic trajectory is exponential in nature (no coupling to the heat bath). This has been proved to be an important manifestation of semiclassical chaos, and is accounted for by using classical arguments and Wigner formalism. For example, Fox and Elston [19] have considered a systematic $1/\hbar$ expansion of the Wigner equation, and the growth of the quantum uncertainty has been shown to depend only on the contribution of classical motion to the Wigner equation, quantum dynamics being subtly involved in the sense that the minimum uncertainty product puts a constraint on the initial Wigner density (so that it is not just a δ function). (See also Ref. [27].) The essential content of the present treatment is that this growth of phase space volume (measured in terms of the uncertainty product or entropy) continues without perceiving the influence of the environment.
[19] R. F. Fox and T. C. Elston, Phys. Rev. B **49**, 3683 (1994).
[20] G. Casati, B. V. Chirikov, F. M. Izraliev, and J. Ford, in *Stochastic Behavior in Classical and Quantum Systems*, edited by G. Casati and J. Ford, Lecture Notes in Physics Vol. 93 (Springer-Verlag, Berlin, 1979), p. 334.
[21] S. Fishman, D. R. Grempel, and R. E. Prange, Phys. Rev. Lett. **49**, 509 (1982).
[22] P. Dutta and S. P. Bhattacharyya, Phys. Lett. **A163**, 193 (1992).
[23] W. Bental, N. Moiseyev, S. Fishman, F. Bensch, and H. Korsch, Phys. Rev. E **47**, 1646 (1993).
[24] D. E. Khmelnitskii, Physica B **126**, 235 (1984).
[25] G. Gangopadhyay and D. S. Ray, J. Chem. Phys. **96**, 4693 (1992); F. Haake, H. Risken, C. Savage, and D. F. Walls, Phys. Rev. A **34**, 3969 (1986).
[26] G. Gangopadhyay and D. S. Ray, Phys. Rev. A **46**, 1507 (1992).
[27] S. Chaudhuri, G. Gangopadhyay, and D. S. Ray, Phys. Rev. E (to be published).